Poultry Science®

Genome-wide mapping of the binding sites of myocyte enhancer factor 2A in chicken primary myoblasts

Xinglong Wang,[*,1] Jiannan Zhang,[*,1] Jiancheng Su,[*] Tianjiao Huang,[*] Ling Lian,[†] Qinghua Nie,[‡] Xin Zhang,[§] Juan Li,[*,§] and Yajun Wang[*,§,2]

[*]*Key Laboratory of Bio-Resources and Eco-Environment of Ministry of Education, College of Life Sciences, Sichuan University, Chengdu 610065, PR China;* [†]*National Engineering Laboratory for Animal Breeding and MOA Key Laboratory of Animal Genetics and Breeding, College of Animal Science and Technology, China Agricultural University, Beijing, PR China;* [‡]*Lingnan Guangdong Laboratory of Agriculture, South China Agricultural University, Guangzhou, PR China; and* [§]*Joint Nutrition Center for Animal Feeding of Sichuan University-Shengliyuan Group*

ABSTRACT Myocyte enhancer factor 2A (**MEF2A**) is a transcription factor that plays a critical role in cell proliferation, differentiation and apoptosis. In contrast to the wide characterization of its regulation mechanism in mammalian skeletal muscle, its role in chickens is limited. Especially, its wide target genes remain to be identified. Therefore, we utilized Cleavage Under Targets and Tagmentation (**CUT&Tag**) technology to reveal the genome-wide binding profile of MEF2A in chicken primary myoblasts thus gaining insights into its potential role in muscle development. Our results revealed that MEF2A binding sites were primarily distributed in intergenic and intronic regions. Within the promoter region, although only 8.87% of MEF2A binding sites were found, these binding sites were concentrated around the transcription start site (**TSS**). Following peak annotation, a total of 1903 genes were identified as potential targets of MEF2A. Gene Ontology (**GO**) enrichment analysis further revealed that MEF2A target genes may be involved in the regulation of embryonic development in multiple organ systems, including muscle development, gland development, and visual system development. Moreover, a comparison of the MEF2A target genes identified in chicken primary myoblasts with those in mouse C2C12 cells revealed 388 target genes are conserved across species, 1515 target genes are chicken specific. Among these conserved genes, ankyrin repeat and SOCS box containing 5 (***ASB5***), transmembrane protein 182 (***TMEM182***), myomesin 2 (***MYOM2***), leucyl and cystinyl aminopeptidase (***LNPEP***), actinin alpha 2 (***ACTN2***), sorbin and SH3 domain containing 1 (***SORBS1***), ankyrin 3 (***ANK3***), sarcoglycan delta (***SGCD***), and ORAI calcium release-activated calcium modulator 1 (***ORAI1***) exhibited consistent expression patterns with MEF2A during embryonic muscle development. Finally, *TMEM182*, as an important negative regulator of muscle development, has been validated to be regulated by MEF2A by dual-luciferase and quantitative real-time PCR (**qPCR**) assays. In summary, our study for the first time provides a wide landscape of MEF2A target genes in chicken primary myoblasts, which supports the active role of MEF2A in chicken muscle development.

Key words: myocyte enhancer factor 2A, binding site, chicken, myoblast

2024 Poultry Science 103:104097
https://doi.org/10.1016/j.psj.2024.104097

INTRODUCTION

Myocyte enhancer factor 2 transcription factors (**MEF2**) are critical regulators in muscle development and function (Black and Olson, 1998a,b; Potthoff and Olson, 2007). In vertebrates, MEF2 are composed of 4 distinct subtypes, namely *MEF2A, MEF2B, MEF2C*, and *MEF2D*, each with similar anatomical and structural organization (Black and Olson, 1998a; McKinsey et al., 2002). Each subtype contains a conserved MADS domain and MEF2 domain at the N-terminal, with a transcriptional activation domain at the C-terminal. The core structure domains (MADS domain and MEF2 domain) mediate MEF2 protein dimerization, cofactor interaction and binding to a cognate cis element with the consensus sequence (T/C)TA(A/T)$_4$TA(G/A) present in the promoters of many muscle and non-muscle specific genes

Received May 3, 2024.
Accepted July 9, 2024.

[1]These authors contributed equally to this work and are considered equal first authors.

[2]Corresponding author: cdwyjhk@163.com

(McDermott et al., 1993; Molkentin et al., 1996a,b; Black and Olson, 1998a; Santelli and Richmond, 2000) .

Among the MEF2 family members, MEF2A is crucial for muscle differentiation and development (Kaushal et al., 1994; Estrella et al., 2015). Adult MEF2A-null mice showed impaired muscle regeneration in response to injury because of a failure of satellite cell-derived myoblasts to differentiate and fuse into multinucleated myotubes (Snyder et al., 2012). The early activation of *MEF2A* expression in the skeletal and cardiac muscle lineages during muscle development is essential for the regulation on the expression of numerous muscle-specific enzymes, structural proteins, and other transcription factors, such as muscle creatine kinase, myosin, tropomyosin, and muscle basic helix-loop-helix protein (Ferrari et al., 1997; Yang, 2000). A majority of MEF2A-knockout mice experienced sudden death accompanied by severe muscle fiber disarray within a week after birth (Naya et al., 2002), providing further evidence of the crucial role of *MEF2A* in muscle development. In addition, mutations or dysregulation of MEF2A are associated with various muscle diseases (Wang et al., 2003; Bachinski et al., 2010; Chen et al., 2017; Nath et al., 2020). For example, a loss-of-function mutation in human MEF2A caused myocardial infarction (Wang et al., 2003). MEF2A-knockout mice exhibited pronounced dilation of the right ventricle (Naya et al., 2002). Although the role of *MEF2A* has been extensively studied in mammals, the role it potentially plays in chicken remains largely unknown.

Transcription factors (**TF**) play their roles through controlling the multiple targets genes in time- and spatial-specific manner (Latchman, 1997). The identification of potential binding sites for TF leads to the promising path for their role revelation, thus drawing wide attention. In recent years, with the continuous development of high-throughput sequencing techniques, various methods have been developed to study DNA binding sites of transcription factors. The in vitro methods, such as DNA immunoprecipitation with microarray detection (**DIP-chip**) (Liu et al., 2005), systematic evolution of ligands by exponential enrichment sequencing (**SELEX-seq**) (Tuerk and Gold, 1990) and protein binding microarrays (**PBM**) (Berger and Bulyk, 2009), allow researchers to study TF-DNA interactions under controlled conditions. However, owing to their in vitro conditions, the important epigenetic and chromatin context effects may be missed. Thus, within the in vivo system, chromatin immunoprecipitation followed by high-throughput sequencing (**ChIP-seq**) (Park, 2009), Cleavage Under Targets and Release Using Nuclease (**CUT&RUN**) (Skene and Henikoff, 2017) and Cleavage Under Targets and Tagmentation (**CUT&Tag**) (Kaya-Okur et al., 2019) now become the focus. These approaches enable researchers to identify genomic targets of TF with high confidence in their natural chromatin context. CUT&RUN and CUT&Tag techniques offer improved repeatability and reduced background noise compared to traditional ChIP-seq methods. This is largely due to their ability to directly target proteins bound to DNA in situ, resulting in more precise and efficient capture of chromatin-associated proteins. Furthermore, the absence of formaldehyde cross-linking and sonication steps in CUT&RUN and CUT&Tag also simplifies the experimental procedure, leading to faster and more efficient workflows. As a result, these innovative techniques have emerged as powerful alternatives for studying chromatin biology and epigenetic regulation.

In human and mouse, the genome-wide binding profiles of MEF2A have been investigated in various tissues, including muscle (He et al., 2011; Wales et al., 2014), bone marrow, brain, blood (Gertz et al., 2013), colon, and cortical neurons (Yan et al., 2013) using ChIP-seq and its derived techniques. In contrast to the extensive characterization of MEF2A target genes in mammalian species, there is currently no established MEF2A binding profile in birds. Among birds, chicken serves as a well-established amniote model for studying skeletal muscle formation and is one of the most popular species in poultry farming (Berti et al., 2015; Ouyang et al., 2017). Hence, our study used CUT&Tag technology to identify MEF2A target genes in chicken skeletal muscle. Because the commercial chicken muscle cell line is not available, chicken primary myoblasts isolated from leg muscles were used. Our study aimed to obtain a detailed view of MEF2A binding landscape, offer a more in-depth understanding of the regulatory role of MEF2A in gene expression during chicken muscle development, and provide the molecular basis for breeding traits that can benefit poultry farming.

MATERIALS AND METHODS

Ethics Statement

All animal experimental protocols performed in this study were approved by the Animal Ethics Committee of the College of Life Sciences, Sichuan University, China, and the assurance number is 20210308008.

Isolation and Culture of Chicken Primary Myoblasts

Chicken primary myoblasts were isolated and cultured as previously described (Wang et al., 2022). Briefly, the leg muscles obtained from three 10.5-day-old embryos of red jungle fowl (Quanfang Poultry Co., Ltd., Pengzhou, China) were cut into small pieces in a 50 mL centrifuge tube and then digested with trypsin (Gibco, Grand Island, NY) at 37°C. The single cell suspension was obtained through filtration using a 70 μm sieve. After the centrifugation at 1,000 × g for 5 min at room temperature, the cell pellet was resuspended in DMEM supplemented with high glucose, 20% (vol/vol) fetal bovine serum (**FBS**) (HyClone, Logan, UT), 100 U/mL penicillin G, and 100 g/mL streptomycin (Life Technologies, Inc., Grand Island, NY). The cells were then seeded in a 10 cm cell culture dish with the fibroblasts remove through 3 differential attachment steps. The cells

were passaged every 2 to 3 d, maintained at less than 80% confluency, and cultured at 37°C with 5% CO_2.

CUT&Tag Assay and Data Analysis

Following Henikoff's study (Kaya-Okur et al., 2019), we selected one sample for the control group and 2 biological replicates for the trial group. A total of 1×10^5 CPMB cells per sample were gently mixed with 100 μL Wash buffer (TD904, Vazyme Biotech, Nanjing, China) and incubated with 10 μL ConA Beads (TD904, Vazyme Biotech) for 10 min at room temperature. After incubation, wash buffer was removed using a magnetic separation rack, and the sample was subsequently incubated with 50 μL primary antibody (diluted 1:200 in Antibody buffer) at 4°C overnight. Since the use of a positive control group is not strictly necessary, present study included only a negative control group and a trial group. The negative control group utilized Rabbit IgG (GB111738, Servicebio Co., Ltd., Wuhan, China), while the trial group employed the Anti-MEF2A Rabbit pAb (GB11965, Servicebio Co., Ltd., Wuhan, China). After primary antibody incubation, the cells were treated with 50 μL secondary antibody (diluted 1:100 in Dig-wash buffer) at room temperature for 1 h, followed by 3 washes with Dig-wash buffer. Subsequently, the cells were incubated with 100 μL pA-Tn5 transposase (diluted 1:50 in Dig-300 buffer) at room temperature for 1 h and washed 3 times with 200 μL Dig-300 buffer. Following this, the cells were incubated with 50 μL TTBL (diluted 1:4 in Dig-300 buffer) for 1 h at 37 °C. Mixed complexes were treated with 2 μL 10% SDS, 30 μg proteinase K, and 1 μL spike -in (DNA fragment of E. coli), and incubated at 55 °C for 10 min. Subsequently, the supernatant was transferred to 50 μL DNA Extract Beads Pro (TD904, Vazyme Biotech) and incubated for 20 min, followed by 2 washes with 200 μL 1 × B&W buffer for 30 s each. DNA was fully eluted with 20 μL ddH_2O and half of the eluted DNA was mixed with 5 μL Stop buffer (TD904-C1, Vazyme Biotech) and incubated at 95°C for 5 min. The CUT&Tag-qPCR was then performed using the gene-specific primers listed in Table S1 and the Bio-Rad CFX96 Real-Time PCR detection system. The other half of the eluted DNA was used for amplification using 2× CAM (TD904, Vazyme Biotech). Amplification products were purified using VAHTS DNA Clean Beads (N411, Vazyme Biotech) and sequenced on Illumina HiSeq PE150 at Novogene Co. Ltd. (Beijing, China). The raw sequencing data have been deposited in China National Center for Bioinformation (**CNCB**) Genome Sequence Archive (**GSA**) and are accessible through GSA series accession number CRA017563 (https://ngdc.cncb.ac.cn/gsa/browse/CRA017563).

Raw sequencing reads were pre-processed using Trim Galore software (version 0.6.7) with the following parameters: -q20, −phred33, −length35, −stringency3, −paired. Subsequently, BWA-MEM (version 0.7.17-r1188) with default parameters was used to align the reads to the *gal6* and *E. coli* reference genome, respectively. Later, duplicated reads were eliminated using Picard tools (version 2.7.3). All aligned reads were normalized using Bedtools (version 2.30.0) with a scaling factor based on the number of reads aligned to the *E. coli* genome, known as spike-in calibration (Egan et al., 2016). A scaling factor S was calculated using the following formula: S = C/(fragments mapped to *E. coli* genome), where C was set at 1,000,000. The generated bam files were converted to bigwig files using "bamCoverage" function from deepTools (Ramírez et al., 2014) in order to visualize them using IGV software (version 2.16.0). Peaks were detected using SEACR software (version 1.3) with parameters "non" (non-normalized) and "stringent" (stringent threshold). Because the utilization of a polyclonal antibody led to increased background noise thus complicating peak recognition, in the present study, the stringent threshold filtering was implemented. Furtherly, through bedtools intersect command with the parameter -f 0.80 and -r, only the regions where peaks from 2 biological replicates mutually overlap by at least 80% are retained. These overlap regions were designated as peaks for further analyses.

For peak annotation, we calculated the distance between peaks and the nearest transcription start site (**TSS**) of all annotated genes using the "annotatePeak" function from the "ChIPseeker" R package (version 1.36.0) (Yu et al., 2015). Peaks surrounding the TSS are frequently indicative of binding regions between transcription factors and genes, which play a critical role in gene activation and expression. By focusing on these regions, we were able to investigate the regulatory mechanism of MEF2A on genes in depth. Therefore, we filtered out peaks that were located beyond 2,000 base pairs upstream and downstream of the TSS and only retained those peaks that were in close proximity to the TSS. Subsequently, for the retained peaks, we utilized Bedtools (version 2.30.0) to extract DNA sequence information.

For motif analysis, the RSAT tool (http://rsat.sb-roscoff.fr/) (Thomas-Chollier et al., 2012) was employed in the present study. We utilized the obtained MEF2A binding motif to validate the presence of the relevant binding site within each peak region. Consequently, peaks lacking the MEF2A binding motif were excluded. Ultimately, the peaks that satisfied both the proximity to TSS and presence of MEF2A binding motif criteria were annotated to their closest genes.

Functional Enrichment Analysis of MEF2A Target Genes

Gene functional annotation was performed using gene symbols obtained from the UniProt database (https://www.ebi.ac.uk/uniprot/). To identify enriched biological processes and pathways, we conducted gene ontology (**GO**) and Kyoto Encyclopedia of Genes and Genomes (**KEGG**) enrichment analysis using the "clusterProfiler" R package (version 4.2.2) (Yu et al., 2012). Gene ontology terms and pathways with a p-value less than 0.05 are considered significantly enriched.

Tissue Expression Analysis of MEF2A Target Genes

Based on the multi-tissue gene expression database of domestic chickens established by our previous studies (https://chickenatlas.avianscu.com/) (Zhang et al., 2022a), we extracted the transcripts per million (**TPM**) values of MEF2A target genes from 35 different chicken tissues, including the brain, midbrain, cerebellum, hindbrain, hypothalamus, tongue, crop, proventriculus, gizzard, duodenum, jejunum, ileum, cecum, rectum, pituitary, spinal cord, pineal gland, retina, heart, liver, spleen, lung, kidney, muscle, skin, fat, bursa of Fabricius, pancreas, thymus, adrenal gland, thyroid gland, parathyroid gland, infundibulum, magnum, and uterus. Subsequently, based on the expression patterns of these genes across different tissues, MEF2A target genes were subjected to clustering analysis using the "pheatmap" R package and visualized using a heatmap. According to the clustering results, the genes within different clusters were subjected to KEGG pathway enrichment analysis using the "clusterProfiler" R package (Yu et al., 2012).

Weighted Gene Coexpression Network Analysis

To identify target genes coexpressed with MEF2A during muscle development in domestic chickens, we downloaded transcriptome data of chicken breast muscle at different developmental stages from the Genome Sequence Archive database with accession number CRA001334 (https://ngdc.cncb.ac.cn/search/?dbId=gsa&q=CRA001334). The dataset comprised 27 samples from 9 developmental stages: embryonic day (**E**)12, E17, 1 d after hatching (**D01**), D07, D21, D56, D98, D140, and D180, each with 3 biological replicates. Using Trim Galore software (version 0.6.7) with the following parameters: -q25, −phred33, −length35, −stringency3, −paired, we filtered the raw data to remove low-quality reads and adapter contamination, aiming to obtain clean data. Subsequently, Salmon software (version 1.6.0) (Patro et al., 2017) with default parameters was used to align the resulting clean data to the chicken reference transcriptome GRCg6 (Gallus_Gallus.GRCg6a.cdna.all.fa) from the Ensembl database. The relative transcript abundances were quantified as TPM values. Samples that could not be distinguished from other time points through principal component analysis were excluded. After ranking the genes according to the median absolute deviation from the highest to the lowest, the top 60% genes were selected for analyses using the "WGCNA" R package (Langfelder and Horvath, 2008). Subsequently, the power parameters ranging from 1 to 20 were screened using the "pickSoftThreshold" function, and the β value (soft threshold) was set as an empirical value of 9 because the scale-free R2 did not exceed 0.8. One-step network construction and module detection were taken using the parameters "minModuleSize" of 30 and "mergeCutHeight" of 0.25. In the present study, we focused the module that contained *MEF2A* in an effort to target the genes co-expressed with *MEF2A* during muscle development. Genes with gene significance >0.6 and module membership > 0.8 were recognized as the hub genes. Finally, a coexpression network was established using Cytoscape (version 3.9.1) (Shannon et al., 2003) software for visualization, based on these hub genes.

Comparative Analysis of MEF2A Target Genes in Chicken and Mice

In our study, we downloaded the MEF2A target gene of mouse C2C12 cells from the Gene Expression Omnibus database according to accession number GSE61204 (https://www.ncbi.nlm.nih.gov/geo/query/acc.cgi?acc=GSE61204) (Wales et al., 2014). Subsequently, the "VennDiagram" R package (Chen and Boutros, 2011) was employed to visualize the overlap between MEF2A target genes in chicken and mice. Finally, the "clusterProfiler" R package was used to conduct GO and KEGG enrichment analysis for species-conserved and species-specific target genes, respectively.

Plasmids Construction

Transmembrane protein 182 ***(TMEM182)*** promoter-reporter plasmids: the chicken *TMEM182* promoter fragment was isolated through PCR using the primers mentioned in Supplementary Table S1. All primers used in this study were synthesized by Youkang Biotechnology (Chengdu, China). The PCR products were subsequently cloned into the pGL3-basic vector to generate the pGL3-cTMEM182 plasmid. Subsequently, we utilized JASPAR (https://jaspar.genereg.net/, threshold set to 0.8) (Castro-Mondragon et al., 2022) and AnimalTFDB3.0 (http://bioinfo.life.hust.edu.cn/AnimalTFDB#!/) databases (Hu et al., 2019) to predict the MEF2A binding site in the *TMEM182* promoter region. For more accurate estimates, only binding sites that turned up in both databases were designated as potential MEF2A binding sites in this study. Based on the prediction results, site-directed deletion of binding site 1 and binding site 2 was carried out through PCR amplification using the specified primers in Supplementary Table S1 and pGL3-cTMEM182 plasmid as a template. This resulted in the generation of 3 *TMEM182* promoter-reporter plasmids with deletion mutations of MEF2A binding sites (pGL3-cTMEM182-del-1, pGL3-cTMEM182-del-2, and pGL3-cTMEM182-del-1&2: both binding sites were deleted.)

MEF2A knockdown plasmid: 3 short hairpin RNA (**shRNA**) (shMEF2A-1, shMEF2A-2, and shMEF2A-3) were designed using BLOCK-iT RNAi Designer (https://rnaidesigner.thermofisher.com/rnaiexpress/) to specifically target chicken *MEF2A*. These short hairpin RNA were then cloned into the pLKO.1-TRC vector to generate the pLKO.1-shMEF2A-1, pLKO.1-shMEF2A-2, and pLKO.1-shMEF2A-3 constructs. As a

negative control, a scramble shRNA (**shSCR**) with no homology to any chicken gene was also cloned into the pLKO.1-TRC vector.

MEF2A overexpression plasmid: the coding sequence for *MEF2A* (NCBI reference sequence: XM_416920.8) was amplified from chicken muscle cDNA through PCR using the primers mentioned in Supplementary Table S1. The PCR product was then cloned into the pcDNA3.1 (+) vector to obtain the overexpression vector (pcDNA3.1-cMEF2A).

Dual-Luciferase Reporter Assay

DF-1 cells, purchased from the American Type Culture Collection (ATCC, Manassas, Virginia), were seeded in a 48-well plate at a density of 1×10^5 cells per well 1 d before transfection. When the cells reached 70% confluence, a mixture containing 100 ng of *TMEM182* promoter-reporter plasmid, 100 ng of *MEF2A* overexpression plasmid (pcDNA3.1-cMEF2A), 5 ng of pRL-TK plasmid, and 0.5 μL of Hieff Trans Liposomal Transfection Reagent (40802ES03, Yeasen Biotechnology Co., Ltd., Shanghai, China) were prepared and transfected following the manufacturer's instructions. After 48 h of transfection (4 repeats for each group), cells were washed by PBS twice and 100 μL of 1× passive lysis buffer (Promega) were added to each well. Luciferase activities of 15 μL of cellular lysates were measured by using Dual-luciferase Assay Kit (Promega) as described previously (Zhang et al., 2022b).

Knockdown of MEF2A by Lentivirus-Mediated shRNA in CPMB

To evaluate the efficiency of the designed shRNA interference, DF-1 cells were seeded at a density of 2×10^5 cells per well in 12-well plates in DMEM supplemented with 10% FBS and incubated for 24 h. Subsequently, the pcDNA3.1-cMEF2A plasmid was respectively co-transfected with 3 interference plasmids, pLKO.1-shMEF2A-1, pLKO.1-shMEF2A-2, and pLKO.1-shMEF2A-3, as well as a control plasmid pLKO.1-shSCR, all in a 1:1 ratio using the Hieff Trans Liposomal Transfection Reagent, following the instructions provided in the manual. After 48 hours of transfection (3 repeats for each group), the whole-cell lysate was subjected to western blot analysis to examine the expression level of MEF2A protein.

For lentivirus packaging, HEK-293 cells (purchased from ATCC) were seeded into a 6-well plate at a density of 5×10^3 cells per well and incubated at 37 °C in a 5% CO_2 environment until reaching approximately 80% confluency in preparation for transfection. Subsequently, 1,000 ng of recombinant lentiviral vector targeting *MEF2A* (experimental group) or pLKO.1-shSCR plasmid (control group) was co-transfected with 900 ng of psPAX2 plasmid and 100 ng of pMD2.G plasmid into the cells. The transfection process was performed using Hieff Trans Liposomal Transfection Reagent, following the provided instructions. After 72 h of transfection, the culture media containing recombinant lentivirus were collected, and stored at -80°C for further studies after centrifuge and filtration.

For lentiviral infection, CPMB were seeded into a 12-well plate at a density of 3×10^4 cells per well. When the cells reached 80% confluence, the prepared recombinant lentivirus was added into the culture medium. The effect of the lentiviral infection was increased by adding polybrene (8 μg/mL). After 48 hours of infection (3 repeats for each group), stable transfected cell lines were selected by adding puromycin (2 μg/mL) to the culture medium. Subsequently, total RNA was extracted from these cells to assess gene expression.

Overexpression of MEF2A in CPMB

In 12-well plate, CPMB were plated at a density of 3×10^4 cells per well. Upon reaching 80% confluence, the cells were transiently transfected with 1 μg of pcDNA3.1-cMEF2A or pcDNA3.1-EGFP vector using Hieff Trans Liposomal following the manufacturer's instructions. After 48 h of infection (3 repeats for each group), cells were harvested. Half of the cells were lysed for subsequent western blot analysis to detect the expression level of MEF2A protein. The other half of the cells were used for total RNA extraction to detect the expression of the target genes of interest.

Western Blot

In brief, the concentrated conditional media were separated on 15% SDS-PAGE gels (Yamei, Shanghai) and transferred to a polyvinylidene difluoride membrane (Sigma-Aldrich, St. Louis, MO). The membrane was incubated in 5% nonfat dry milk for 2 h at room temperature to block nonspecific protein binding. Next, the membrane was washed 3 times with TBST, followed by incubation with anti-MEF2A primary antibody (1:2,000, GB11965, Servicebio) at 4°C overnight. After washing 3 times with TBST, the membrane was incubated with HRP-conjugated goat anti-mouse secondary antibody (1:5,000, A9044, Sigma) for 2 h at room temperature. The blots were then visualized using an ECL chemiluminescence detection kit following manufacturer's instruction (Thermo Fisher Scientific, Waltham, MA).

Total RNA Extraction, Reverse Transcription and Quantitative Real-time PCR Assay

Total RNA was prepared from CPMB by RNAzol reagent (Molecular Research Center, Cincinnati, OH) according to the manufacturer's protocol. Briefly, the cells were lysed in RNAzol and then precipitated with diethylpyrocarbonate (**DEPC**)-treated ultra-pure water before being centrifuged at 12,000 rpm for 10 min. To purify the RNA and remove genomic DNA, 4-bromoanisole (**BAN**) solution was added and then followed by an equal volume of cold isopropanol. The resulting pellet was washed 3 times with 200 μL of 75% ethanol

and dissolved in 10 μL of RNase-free water. The concentration and purity of the samples were measured using a Onedrop1,000 Spectrophotometer.

In the present study, total RNA was used for cDNA synthesis by reverse transcription, using M-MLV reverse transcriptase (Takara, Dalian, China) as described previously (Lv et al., 2022). Briefly, 2 μg of total RNA and 0.5 μg of oligo-deoxythymidine were heated at 70°C for 10 min, chilled at 4 °C for 2 min to bring the volume to 5 μL, and then supplemented with the first-strand buffer, 0.5 mM of each deoxynucleotide triphosphate, and 100 U of M-MLV reverse transcriptase, resulting in a final volume of 10 μL. Reverse transcription was performed at 42 °C for 90 min.

Expression of *MEF2A* and *TMEM182* mRNA was analyzed using qPCR, according to our previous study (Fang et al., 2021). The reaction mixture was composed of 10 μM primers, 10 mM dNTP, easy Taq buffer, easy Taq DNA polymerase (TransGen Biotech), Eva Green (Biotium), MilliQ-H_2O, and templates, in a total volume of 20 μL. The reaction was conducted on the Bio-Rad CFX96 Real-Time PCR detection system, with an initial denaturation at 94°C for 10 min, followed by 40 cycles of denaturation at 94°C for 20 s, annealing at 60°C for 15 s, and extension at 72 °C for 30 s. The specificity of qPCR amplification was determined by conventional PCR and gel electrophoresis with melting curve analysis after qPCR. The mRNA expression levels of *MEF2A* and *TMEM182* were calculated using the $2^{-\Delta\Delta CT}$ relative quantitation method, normalized to the β-actin gene, and expressed as fold-differences versus the negative control.

Statistics Analysis

The mRNA level of each gene was first normalized by that of β-actin and then expressed as fold difference compared to the control group. Luciferase activity of promoter-luciferase construct in DF-1 cells was normalized to Renilla luciferase activity derived from the pRL-TK vector (Promega) and then expressed as relative fold increase compared with the control group (promoter-less pGL3-Basic vector). Statistical analyses were carried out using GraphPad Prism 7 (Graph Pad Software Inc., San Diego, CA). Student's test was used to compare 2 groups, for more than 2 groups, one-way ANOVA was performed followed by Dunnett's test. All experiments were repeated at least twice to validate the results. Results were considered statistically significant at a P-value of less than 0.05. The following notations indicate levels of significance: $^*P < 0.05$; $^{**}P < 0.01$; $^{***}P < 0.001$.

RESULTS

The Genome-Wide Binding Profiles of MEF2A in CPMB

To obtain the landscape of MEF2A target genes in myogenesis, the CUT&Tag technique was used to generate 3 libraries (MEF2A-rep1, MEF2A-rep2, and IgG) in CPMB. After the high-throughput sequencing, the sequencing depth, mapping rate, and duplication rate of each sample were evaluated (Supplementary Table S2). The PCR duplication rates for the trial (MEF2A-rep1 and MEF2A-rep2) and control (IgG) samples were above 30%, possibly due to the lower complexity of CUT&Tag libraries compared to the conventional libraries. After the duplicates were removed, the length distribution of inserted fragments within the library was analyzed, which exhibited a periodic saw-tooth-like pattern with a 10 bp cycle (Figure 1A).

Due to the lack of commercially available antibodies specific to chicken MEF2A protein, with the conservation of MEF2A across different species (as shown in Figure S1, the chicken MEF2A shared high amino acid sequence identities with that of mouse (94.4%), rabbit (91.8%), and human (93.5%), respectively), a polyclonal antibody raised against mouse MEF2A was adopted in this study for the detection of the chicken ortholog. This might have caused a higher background noise and challenges for peak recognition in data analysis. To address this issue, a more stringent threshold was applied in defining peaks, in which only regions exhibiting > 80% overlap between the peaks of the 2 biological replicates were defined as genuine peaks and subjected to further analyses. A total of 120,336 peaks were identified. Among these peaks, except the 583 peaks located on chr Random and chrUn, which could not be annotated, the remaining 119,753 peaks were successfully annotated by "ChIPseeker" R package (Yu et al., 2015). As shown in Figure 1B, 28.77% of the peaks were located within 10 kb from the TSS, 57.47% of the peaks were situated 10 to 100 kb away from the TSS, and 13.76% of the peaks were located more than 100 kb from the TSS. Furthermore, we explored the peak distribution within the different genomic elements. As shown in Figure 1C, 39.39% and 40.98% of the peaks were respectively located within intergenic and intron regions while 8.87% of the peaks (10617 peaks) were found to be located within the promoter region (2 kb upstream or downstream of the TSS). In addition, these 10617 peaks were found to be enriched around TSS (Figure 1D).

In the present study, the peak-motifs tool RSAT (Thomas-Chollier et al., 2012) (http://rsat.sb-roscoff.fr/) was further employed to perform the de novo motif analysis on the 10,617 peaks in the promoter region. As shown in Figure 1E, the motif with "TAAAAATA" core sequence shared striking similarity with the motif of *MEF2A* in the JASPAR database (k-mer sig = 9.73; e-value = 1.9×10^{-10}; normalized cor = 0.815). Among the 10,617 peaks, 3255 peaks showed at least one such putative MEF2A binding site (Supplementary Table S3) supporting the direct binding of MEF2A with DNA and thus being the focus of the present study. The remaining 7362 peaks harbored alternate motifs such as GATA binding protein 1 (**GATA1**), TEA domain transcription factor 1 (**TEAD1**), nescient helix-loop-helix 1 (**NHLH1**), and ETS variant transcription factor 4 (**ETV4**) motifs (Figure 1F), hinting that MEF2A may

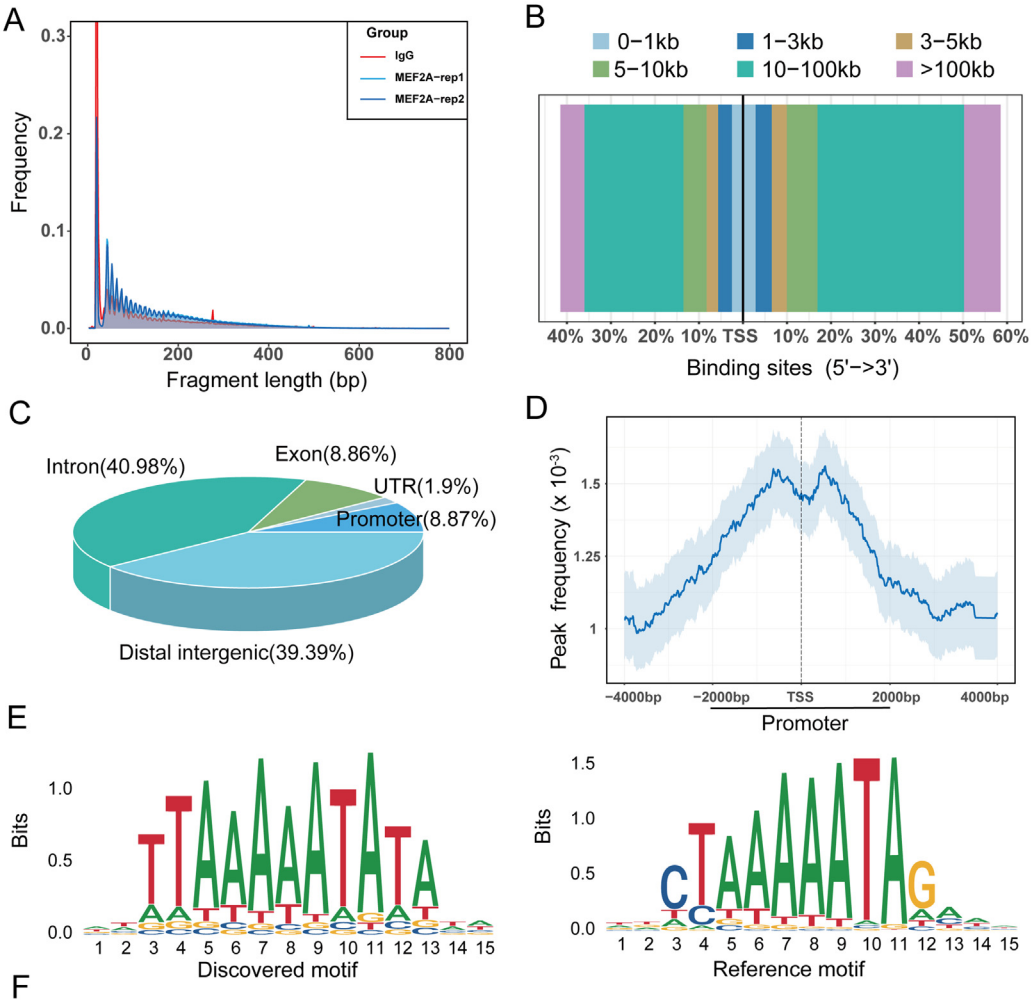

Name	Discovered motif	Reference motif	Ncor	k-mer sig	Evalue
GATA1	rvAGAGAArr	rsWGATAAgrr	0.679	350.00	0
TEAD1	csCATCCCcs	yrCATTCCwy	0.724	4.36	4.4×10^{-05}
NHLH1	ssCGCAGCGss	gCGCAGCTGCKy	0.637	47.90	1.3×10^{-48}
ETV4	ssAGGAGGrr	rcAGGAAGyr	0.759	350.00	0
MZF1	ggAGGGGGAgg	bkAKGGGkrr	0.804	42.32	4.8×10^{-43}
NRF1	csCGCatGCGsg	GCGCmTGCGCr	0.818	21.38	4.2×10^{-22}
CTCFL	ssCGGGGGGCgs	rsCAGGGGGCgs	0.798	19.22	6×10^{-20}

Figure 1. The genome-wide binding profiles of MEF2A in chicken primary myoblasts. (A) Frequency distribution of insert fragment length in CUT&Tag library. (B) Distance distribution of the peaks from the transcription start site (**TSS**). (C) Distribution of the peaks in exons, introns, promoters, intergenic and untranslated regions (**UTR**). (D) Frequency distribution of the peaks in the promoter region. (E) De novo motif analysis of MEF2A-bound genomic regions showing the most enriched sequence motifs (k-mer sig = 9.73; evalue = 1.9×10^{10}; normalized cor = 0.815). (F) De novo motif analysis of *MEF2A*-bound genomic regions showing the other enriched sequence motifs.

also act as a co-factor of other transcription factors and indirectly bind to DNA to regulate gene expression, nevertheless, this still awaits further elucidation which will be included on our next manuscript.

GO and KEGG Enrichment Analyses of MEF2A Target Genes

In order to identify the MEF2A target genes and elucidate their biological processes and pathways involved, the 3,255 peaks harboring MEF2A motifs were used for gene annotation. A total of 2,838 distinct target genes were identified (Supplementary Table S4). After excluding the 935 target genes whose names start with "LOC", the remaining 1903 target genes were subjected for the GO and KEGG analyses. As shown in Figure 2A, these target genes were primarily enriched in the processes related to muscle tissue development. In addition, these target genes were also found to be enriched into the GO terms including embryonic organ development, eye development, visual system development, gland development and regulation of membrane potential. As shown in Figure 2B, KEGG enrichment analysis revealed the involvement of these target genes in key pathways such as calcium signaling pathway (Chin,

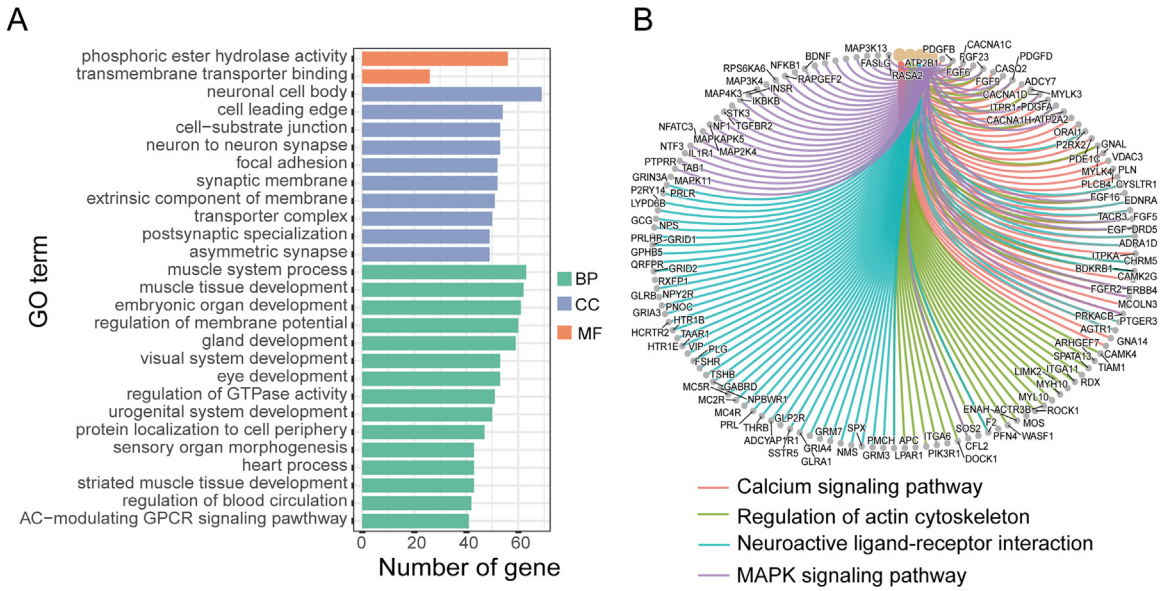

Figure 2. Functional enrichment analysis of MEF2A target genes. (A) The enriched GO terms ($P < 0.05$) of MEF2A target genes were presented according to biological process (**BP**), cellular component (**CC**), and molecular function (**MF**). (B) The enriched KEGG pathways ($P < 0.05$) of MEF2A target genes.

2010; Baylor and Hollingworth, 2011), regulation of actin cytoskeleton (Kee et al., 2009; Tang and Gerlach, 2017), and MAPK signaling pathway (Keren et al., 2006; Segalés et al., 2016).

Tissue Expression Atlas of MEF2A Target Genes

To investigate the expression patterns of MEF2A target genes, we extracted TPM values of MEF2A target genes from 35 different chicken tissues in our previously established multi-tissue gene expression database of chickens (https://chickenatlas.avianscu.com/) (Zhang et al., 2022a). As shown in Figure 3, MEF2A target genes are specifically highly expressed in multiple tissues or systems. For example, 61 genes were highly expressed in the muscular syste, 468 genes in the central nervous system, 139 genes in the intestinal system, and 103 genes in the immune system.

Furthermore, we performed KEGG pathway enrichment analysis on target genes that exhibited high expression in different systems and tissues. As shown in Figure S2, MEF2A target genes with muscle system-specific expression were primarily enriched in the "calcium signaling pathway," those with central nervous system-specific expression were mainly enriched in "neuroactive ligand-receptor interactions," those with digestive system-specific expression were primarily enriched in "drug metabolism - other enzymes," and those with immune system-specific expression were mainly enriched in "cytokine-cytokine receptor interactions," among others. These results revealed functional differences of MEF2A target genes in specific physiological systems and tissues.

Co-expression Analysis of MEF2A and Its Target Genes During Muscle Development

Muscle development relies on the multiple transcription factors to orchestrate cellular processes such as muscle cell proliferation, differentiation, and fusion in a specific spatio-temporal pattern (Taylor and Hughes, 2017). To identify target genes continuously regulated by MEF2A during muscle development, WGCNA analysis was performed on the CRA001334 dataset (https://ngdc.cncb.ac.cn/search/?dbId=gsa&q=CRA001334) (Xing et al., 2020), which contains chicken breast muscle gene expression data at nine developmental stages (E12, E17, D1, D7, D21, D56, D98, D140, and D180). To ensure the validity of the analysis, principal component analysis was performed on the data. As shown in Figure 4A, the samples from the first 5 developmental stages (E12, E17, D1, D7, and D21) were separable from each other, but the samples from the latter 4 developmental stages (D21, D56, D98, D140, and D180) could not be separated and were therefore excluded from further analysis. By applying dynamic tree cut algorithm to the transcriptome data from the first 5 developmental stages, a total of 12 modules were identified (Figure 4B). The brown module (containing *MEF2A* gene) comprised 410 genes, of which 168 genes (module membership > 0.8, gene significance > 0.6) were considered co-expressed with *MEF2A* during muscle development (Figure 4C). Finally, the 168 genes co-expressed with MEF2A were further compared with the identified 1903 MEF2A target genes, and a total of 31 genes (18%) were identified to be targeted by MEF2A (Figure 4D). These target genes are presumed to be continuously regulated by MEF2A during muscle development, thereby influencing the process of muscle development.

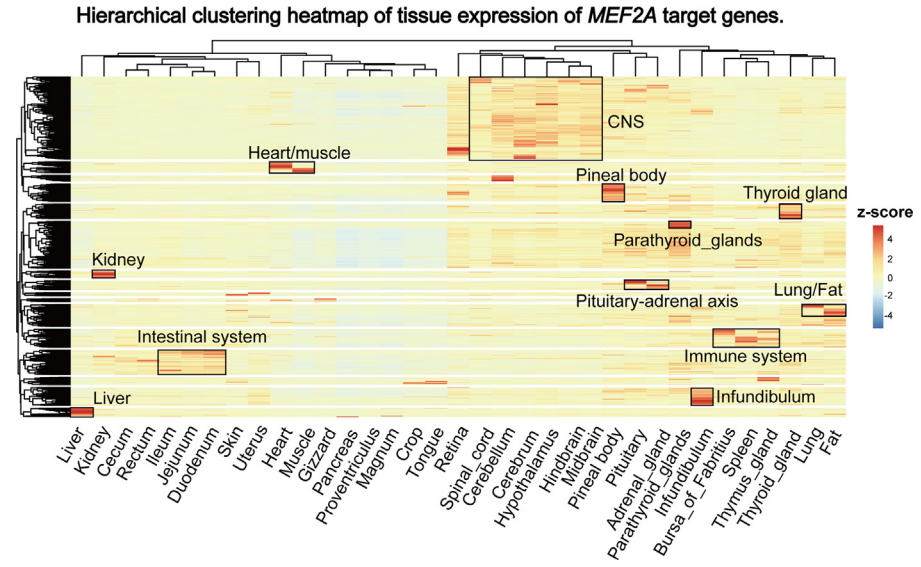

Figure 3. Hierarchical clustering heatmap of tissue expression of MEF2A target genes in chickens. The raw data were downloaded from CNGB Sequence Archive (CNSA) of China National GeneBank DataBase (**CNGBdb**) with accession number CNP0003404, which is publicly accessible for all researchers at https://db.cngb.org/search/project/CNP0003404/.

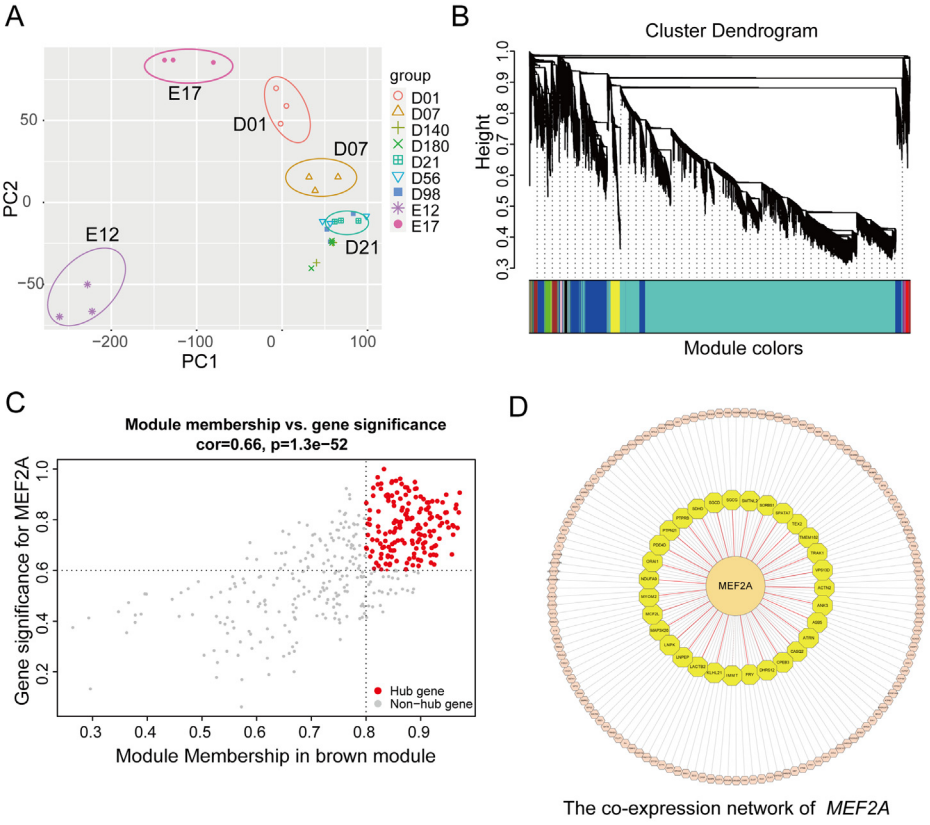

Figure 4. Weighted coexpression network analysis of MEF2A and its target genes during chicken breast muscle development. (A) Principal component analysis of transcriptome data from breast muscle of chicken embryo at different developmental stages. The ellipses represent the distribution of samples within each group and do not serve as confidence ellipses. The raw data were obtained from the China National Center for Bioinformation, under the accession number CRA001334, which is publicly accessible for all researchers at https://ngdc.cncb.ac.cn/search/?dbId=gsa&q=CRA001334 (B) Gene dendrogram obtained by clustering the dissimilarity based on consensus topological overlap with the corresponding module colors indicated by the color row. Each colored row represents a color-coded module which contains a group of highly connected genes. A total of 12 modules were identified. (C) A scatterplot of gene significance (**GS**) for MEF2A vs. module membership (**MM**) in the brown module. The red dots represent points with MM > 0.8 and GS > 0.6. (D) The co-expression network of *MEF2A* and its target genes. All genes on the circle are co-expressed with *MEF2A* during the process of muscle development. The yellow genes located on the inner circle are the target genes of MEF2A recognized by our CUT&Tag data.

Comparative Analysis of MEF2A Target Genes in Chicken and Mouse

Transcriptional regulation plays pivotal roles in evolution. The evolution of phenotypes is frequently linked to variations in transcriptional regulation across different species (King and Wilson, 1975; Bird et al., 2006; Moses et al., 2006). In order to explore the regulatory roles of MEF2A across different species, we performed a comparative analysis between the 1903 MEF2A target genes identified through our CUT&Tag analysis in CPMB and the 3,121 genes identified through ChIP-exo-seq analysis in the mouse muscle C2C12 cell line (Wales et al., 2014). The comparison revealed a total of 388 conserved MEF2A target genes between the 2 species, with 1,515 genes specific to chicken and 2,733 genes specific to mice (Figure 5A and Supplementary Table S5). Further GO enrichment analysis showed that the conserved target genes between the 2 species are involved in multiple biological processes, including the muscle development, cell differentiation, and signal transduction (Figure 5B). Regarding the chicken-specific target genes, KEGG analysis highlighted their enrichment in "glycerophospholipid metabolism," "starch and sucrose metabolism," and "GnRH signaling pathway" (Figure S3A). Conversely, the mouse-specific target genes were enriched in "Proteoglycans in cancer," "Pathways in cancer," and "Hippo signaling pathway" (Figure S3B).

Identification of Conserved MEF2A Target Genes During Muscle Development

To focus on the conserved MEF2A target genes during muscle development, we performed a comparative analysis between the 388 conserved MEF2A target genes and the 168 co-expressed genes with *MEF2A* identified from WGCNA analysis. As shown in Figures 6A and 6B, a total of 9 conserved genes, namely ankyrin repeat and SOCS box containing 5 (***ASB5***), *TMEM182*, myomesin 2 (***MYOM2***), leucyl and cystinyl aminopeptidase (***LNPEP***), actinin alpha 2 (***ACTN2***), sorbin and SH3 domain containing 1 (***SORBS1***), ankyrin 3 (***ANK3***), sarcoglycan delta (***SGCD***), and ORAI calcium release-activated calcium modulator 1 (***ORAI1***), were found to show the consistent expression profile with *MEF2A* (data from CRA001334, https://ngdc.cncb.ac.cn/search/?dbId=gsa&q=CRA001334), suggesting the potential directive involvement of MEF2A during muscle development. In contrast, the expression patterns of the other 379 MEF2A target genes differed from that of MEF2A (Figure S4), implying the indirective involvement of MEF2A along the developmental stages. The involvement of MEF2A regulation for the other 379 genes may be limited to specific developmental stages or require synergistic regulation from other transcription factors. In the mouse C2C12 cell line, as shown in Figure 6C, knockdown of MEF2A resulted in the decrease in expression levels of these 9 genes (not significance for *LNPEP*) (Estrella et al., 2015), providing evidence for their regulation by MEF2A (data from GSE63798, https://www.ncbi.nlm.nih.gov/geo/query/acc.cgi?acc=GSE63798) Interestingly, among these 9 conserved genes, we observed that the gene *TMEM182* exhibited a specific high expression in muscle (data from CNP0003404, https://db.cngb.org/search/project/CNP0003404/) (Figure 6D).

Validation of TMEM182 as a Target Gene for MEF2A

Among the identified 9 conserved MEF2A target genes, *TMEM182* has been proven to be involved in regulating processes such as muscle differentiation and regeneration (Wu and Smas, 2008; Luo et al., 2021). Therefore, in this study, we further validated the regulatory role of MEF2A on *TMEM182*.

As shown in Figure 7A, a clear peak was detected near the promoter region of *TMEM182*, indicating that MEF2A can bind *TMEM182*. To validate this finding,

Figure 5. Comparative analysis of MEF2A target genes in chicken and mice. (A) The Venn diagram of CUT&Tag data from chicken primary myoblasts and ChIP-exo-seq data from mouse C2C12 cells (data from GSE61204, https://www.ncbi.nlm.nih.gov/geo/query/acc.cgi?acc=GSE61204). (B) The enriched GO terms ($P < 0.05$) of conserved MEF2A target genes between chicken and mice. The terms highlighted in red represent biological processess associated with muscle development.

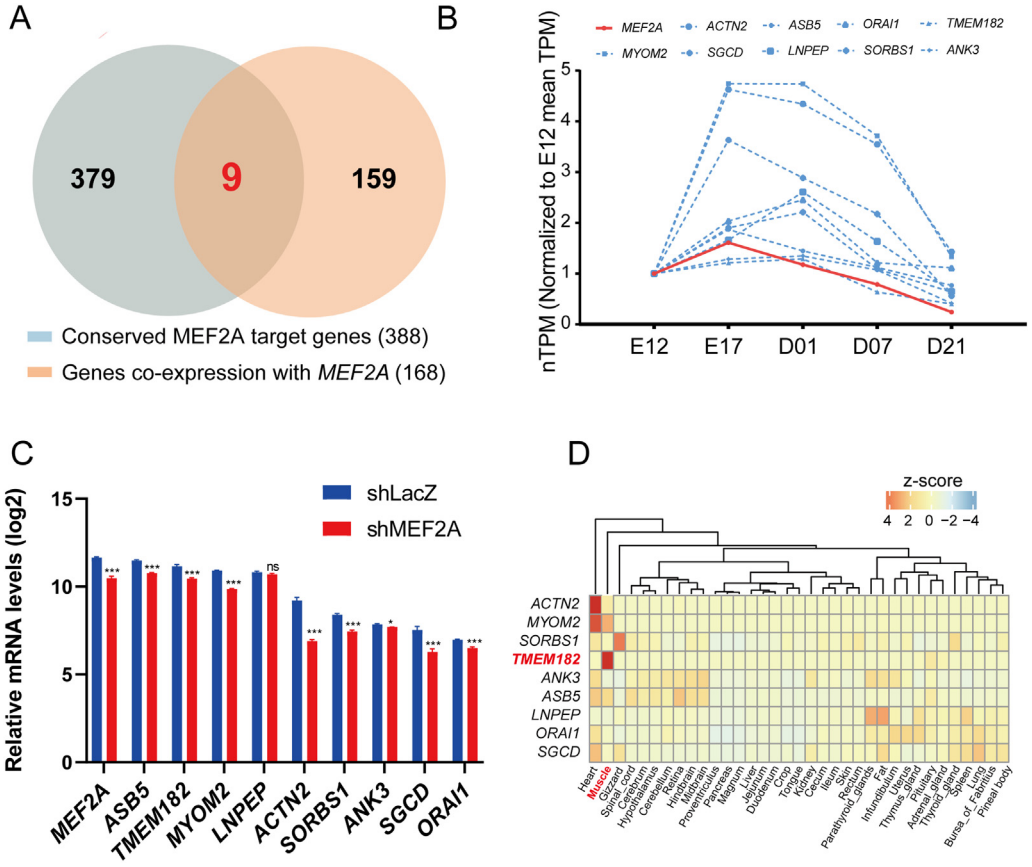

Figure 6. Identification of conserved target genes regulated by MEF2A during breast development. (A) The Venn diagram of the genes co-expressed with *MEF2A* (data from Figure 4) and the species-conserved MEF2A target genes (data from Figure 5) (B) Expression pattern of *MEF2A* and the identified conserved genes during breast muscle development (data from CRA001334, https://ngdc.cncb.ac.cn/search/?dbId=gsa&q=CRA001334). (C) Expression of the 9 conserved genes in C2C12 cells with *MEF2A* knockdown by shRNA ($n = 3$ cultures, mean ± SEM; 2-tailed Student's t-test, $^{*}P < 0.05$; $^{**}P < 0.01$; $^{***}P < 0.001$). The raw data were obtained from Gene Expression Omnibus database, under the accession number GSE63798, which is publicly accessible for all researchers at https://www.ncbi.nlm.nih.gov/geo/query/acc.cgi?acc=GSE63798. (D) Tissue expression profile of the 9 conserved genes in chickens (data from CNP0003404, https://db.cngb.org/search/project/CNP0003404/).

our study utilized the JASPAR (https://jaspar.genereg.net/) (Castro-Mondragon et al., 2022) and AnimalTFDB3.0 (http://bioinfo.life.hust.edu.cn/AnimalTFDB#!/) (Hu et al., 2019) databases to predict MEF2A binding sites within the *TMEM182* promoter region. As shown in Figure 7B, the *TMEM182* promoter region contains 2 potential MEF2A binding sites that are conserved across species. As shown in Figure 7C, 4 different *TMEM182* promoter fragments (wild type, binding site 1 deletion, binding site 2 deletion, and both binding site 1 and 2 deletions) were inserted into the pGL3-Basic vector to construct reporter plasmids. Dual-luciferase reporter assay demonstrated that the expression of MEF2A significantly increased luciferase activity in the wild-type group (containing the wild-type *TMEM182* promoter fragment). Although deletion of either binding site still led to a significant increase in luciferase activity, the fold change was reduced compared to the wild-type group. However, simultaneous deletion of both binding sites abolished the ability of MEF2A to increase luciferase activity. These findings indicate that the *TMEM182* promoter region harbors 2 MEF2A-binding sites. CUT&Tag-qPCR analysis further confirmed that MEF2A can bind to the *TMEM182* promoter region (Figure S5).

To further verify the transcriptional regulation effect of MEF2A on *TMEM182* gene, The BLOCK-iT RNAi Designer software (https://rnaidesigner.thermofisher.com/rnaiexpress/) was used to design 3 shRNA for *MEF2A* knocking down. As shown in Figure S6, western blot analysis showed all 3 shRNA effectively interfered with the exogenous *MEF2A* expression in DF-1 cells, with interference efficiencies of 72.07%, 92.10%, and 76.02%. Subsequently, the 2 shRNA with higher interference efficiencies were packaged into lentiviral particles for infecting CPMB. As expected, the decreased expression levels of *MEF2A* led to a corresponding reduction in *TMEM182* transcription levels (Figure 7D). Conversely, overexpressing the *MEF2A* in CPMB increased the transcriptional levels of *TMEM182* (Figure 7E and Figure S7).

DISCUSSION

In this study, CUT&Tag technology was used to investigate the genome-wide binding profile of MEF2A. The MEF2A target genes were annotated, which showed tissue or system specific expression involving in multiple biological processes and signaling pathways, supporting

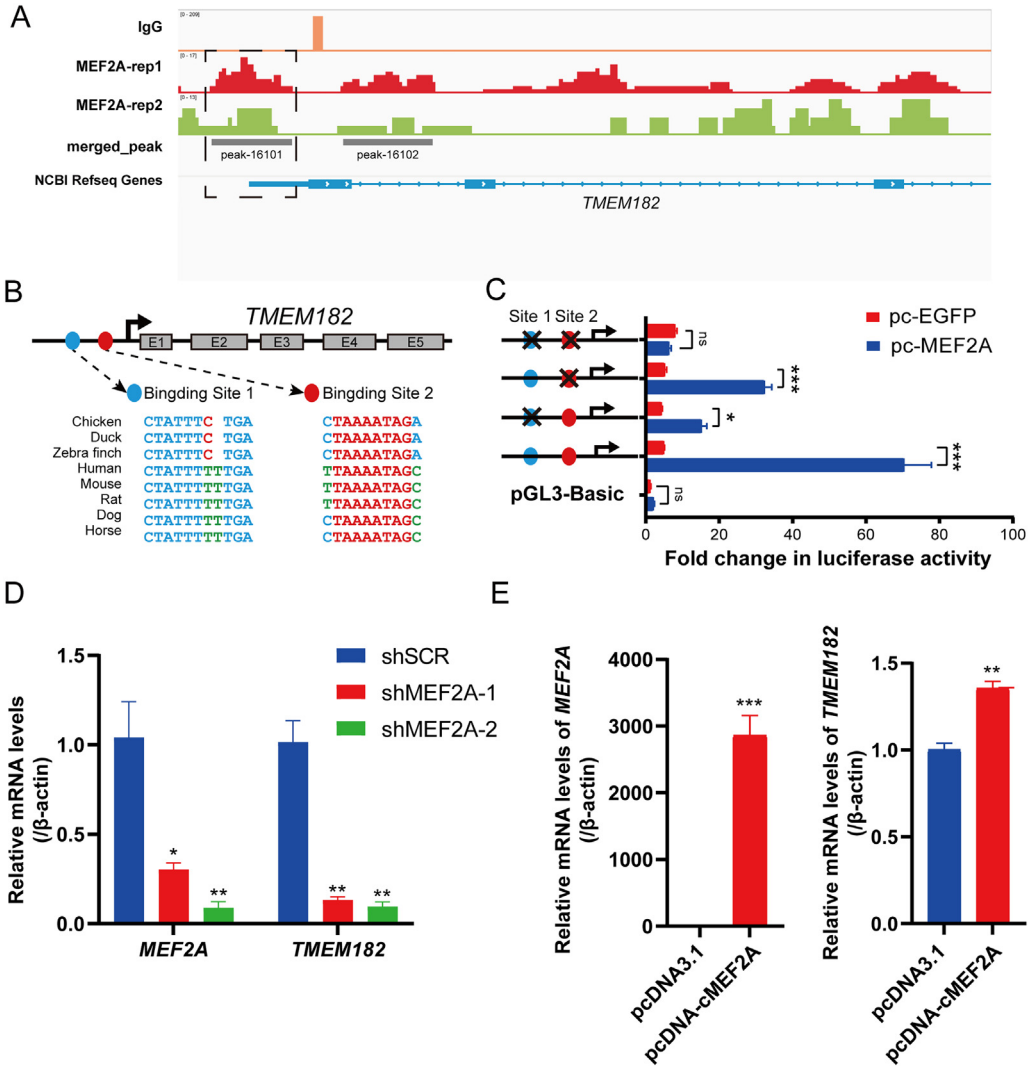

Figure 7. Regulation of *TMEM182* expression by MEF2A. (A) CUT&Tag analysis showing a clear peak near the promoter region of *TMEM182*. (B) The cross-species sequence alignment of MEF2A binding sites predicted by JASPAR and AnimalTFDB3.0 databases. (C) Luciferase activity of *TMEM182* promoter containing wild-type, binding site 1 deletion, binding site 2 deletion, and both binding sites 1 and 2 deletion ($n = 4$ cultures; mean ± SEM, 2-tailed Student's t-test). The mRNA levels of *MEF2A* and *TMEM182* in chicken myoblasts after MEF2A knockdown (D) and overexpression (**E**) ($n = 3$ cultures; mean ± SEM; 2-tailed Student's t-test). $^{*}P < 0.05$; $^{**}P < 0.01$; $^{***}P < 0.001$.

the broad regulatory role of MEF2A. The co-expression network and cross-species comparative analysis set the successful examples to annotate MEF2A target genes which support the important regulatory role of MEF2A in chicken muscle development.

Our study found that a significant proportion of the peaks were localized within the intergenic and intronic regions. This finding is consistent with the reports from human and mouse (Gertz et al., 2013; Wales et al., 2014). For example, in mouse cardiomyocytes and skeletal muscle cells, ChIP-seq analysis revealed that over 90% of the binding sites were distributed in intergenic regions and introns (Wales et al., 2014). In human B lymphocytes and neuroblastoma cells, ChIP-seq analysis revealed that over 80% of the binding sites were distributed in intergenic regions and introns (Gertz et al., 2013). One possible explanation is that MEF2A shows the tendency to bind to DNA sequences abundant in A or T nucleotides (Black and Olson, 1998a; Santelli and Richmond, 2000). Generally, regions categorized as intronic and intergenic tend to be more enrich in A or T nucleotides (Rao et al., 2013). Alternatively, MEF2A may bind to the varied enhancers (mainly located in intergenic and introns regions) thus showing more wide distribution within the chicken genome. Although the majority peaks are distributed within intergenic and intronic regions, no evident peaks enrichment were observed within these regions. Conversely, although only 8.87% of the peaks located in the promoter region, these peaks exhibit enrichment around TSS (Figure 1D), supporting the function of MEF2A as a transcription factor capable of binding to the promoter region and, consequently, regulating gene expression.

In the present study, a total of 7362 peaks were found to contain additional motifs such as GATA1, TEAD1, NHLH1, and ETV4, hinting the indirect binding of DNA by MEF2A acting as a co-factor to other transcription factors. This finding supports that the MEF2A, like other MADS-box proteins, may interact with a range of other transcription factors, resulting in the activation of

multiple gene expression (Kaushal et al., 1994; Santelli and Richmond, 2000). For example, the MEF2 proteins have been reported to be recruited to target the promoters for GATA transcription factors to potentiate their transcriptional activities (Morin et al., 2000). In addition, the promoter of atrial natriuretic factor can be activated by cooperation between MEF2A and GATA-1 (Wang et al., 2003). MEF2A and TEAD1 can jointly bind to a subset of gene promoters (Joshi et al., 2017). The present study was also in line with ChIP-seq data from mouse MEF2, where the NHLH1 motif (E-box) was also found (Thomas-Chollier et al., 2012; Amoasii et al., 2019). DNA-binding and luciferase reporter assays demonstrated MEF2 can interact with ETV4 to enhance its transcription activity through conducting (Xiang et al., 2022). The extent of target genes that maybe indirectly bound and regulated by MEF2A propels us to set our course for a more in-depth study to elucidate the potential roles played by MEF2A in our next manuscript.

The identified 1903 MEF2A target genes exhibit high expression in various systems and tissues, providing evidence for the vital role played by MEF2A in multiple physiological processes. Among the target genes highly expressed in the CNS, fibroblast growth factor 9 (***FGF9***) controls the formation of the Bergmann fiber scaffold which is responsible for the inward migration and maturation of Purkinje cells guiding (Lin et al., 2009). Ankyrin 2 (***ANK2***) is associated with axon and synapse formation in neurons (Yang et al., 2019). Vasoactive intestinal peptide (***VIP***) has been shown to stimulate both the proliferation and differentiation of neurons within the brain (Moody et al., 2003). Among the genes highly expressed in the immune system, B and T lymphocyte associated (***BTLA***) can significantly inhibit T cell activation and proliferation (Watanabe et al., 2003). Chemokine receptor 2 (***CCR2***) plays a crucial role in facilitating the recruitment of monocytes and macrophages to the sites of inflammation, as well as their egress from the bone marrow (Boring et al., 1997; Kurihara et al., 1997; Kuziel et al., 1997). Janus kinase 1 (***JAK1***) has been shown to mediate the persistent oncogenic activation of signal transducer and activator of transcription 3 (***STAT3***) in mammary cancer cells (Wehde et al., 2018). Among the genes highly expressed in the intestinal system, Cadherin 1 (***CDH1***) is essential for maintaining the stability of intestinal epithelial cells through cell-cell adhesion and cell polarity (Aitchison et al., 2020). Lactase (***LCT***) is integral to the plasma membrane and has both phlorizin hydrolase activity and lactase activity. Mutations in this gene are associated with congenital lactase deficiency (Kuokkanen et al., 2006). Thus, these tissue-specific target genes reveal the multifaceted functions of MEF2A in various systems supporting that MEF2A plays a crucial role and potentially participates in a wide physiological process.

MEF2A target genes are significantly enriched in processes and pathways related to muscle development and function. For example, "calcium signaling pathway", essential for muscle contraction (Chin, 2010; Baylor and Hollingworth, 2011), "actin cytoskeleton pathway", responsible for maintaining muscle cell structure and facilitating movement (Kee et al., 2009; Tang and Gerlach, 2017), and "MAPK signaling pathway", linked with cell proliferation and differentiation (Keren et al., 2006; Baylor and Hollingworth, 2011), all support the role of MEF2A in muscle development and function. Further evidence supporting the involvement of MEF2A in muscle development comes from cross-species comparisons in chicken and mice. Among the 388 conserved target genes of MEF2A, 9 genes exhibit similar expression patterns to MEF2A throughout muscle development (Figures 6A and 6B). These genes have been previously implicated in muscle development, structure, and function. For example, *MYOM2* is a distinctive structural protein that is exclusively found in muscles and serves to strengthen the sarcomere in proximity to the M-line. *ACTN2*, predominantly expressed in muscle tissue, plays a crucial role as a major structural component of the contractile apparatus located at the Z-line. It functions as a pivotal link between the anti-parallel actin filaments, enabling efficient muscle contraction. Moreover, the binding of *ACTN2* to the N-terminal titin provides support to the sarcomere and significantly contributes to its stability (Lek et al., 2010; Ranta-aho et al., 2022). The high expression of *SORBS1* in the sarcomere suggests that it may function as a scaffolding protein to maintain the structural integrity of the contractile apparatus in skeletal muscle. *SORBS1* may also play a role in the regulation of cytoskeletal dynamics by aiding in the formation of actin stress fibers, which are critical for muscle contraction (Lin et al., 2001; Harney et al., 2005; Sampath et al., 2018).

Our study for the first time reported that MEF2A regulated *TMEM182* mRNA expression. TMEM182 is a negative regulator in muscle differentiation and regeneration, which is reported to be significantly upregulated by MYOD1 during the muscle differentiation (Luo et al., 2021). However, the *TMEM182* mRNA expression reaches its highest level on the fifth day after differentiation, 3 d after the peak expression of myogenic differentiation 1 (***MYOD1***) (Panda et al., 2014; Nie et al., 2017; Hsing et al., 2019; Luo et al., 2021). Thus, the peak expression of *TMEM182* and *MYOD1* are not synchronized. The present finding that *TMEM182* promoter region is targeted by MEF2A supports that MEF2A may coordinate with MYOD1 to regulate the *TMEM182* expression. MEF2A may be involved in regulating the high levels of *TMEM182* following the *MYOD1* decrease. The accumulated TMEM182 protein may interact with ITGB1, thereby influencing downstream signaling pathways ultimately blocking excessive myogenesis. Thus, MEF2A may negatively regulate myogenesis by promoting the expression of TMEM182. However, the specific role of MEF2A in myogenesis and muscle development requires further investigation for its wide target genes.

ACKNOWLEDGMENTS

This work was supported by grants from the National Natural Science Foundation of China (U1901206, 32072706, and 31802056), the Natural Science Foundation of Sichuan Province (2024NSFSC0299 and 2023NSFSC0230), and the Project Funded by China Postdoctoral Science Foundation (2019M653412 and 2020T130439).

DISCLOSURES

The authors declare no conflicts of interest.

SUPPLEMENTARY MATERIALS

Supplementary material associated with this article can be found in the online version at doi:10.1016/j.psj.2024.104097.

REFERENCES

Aitchison, A., C. Hakkaart, M. Whitehead, S. Khan, S. Siddique, R. Ahmed, F. A. Frizelle, and J. I. Keenan. 2020. CDH1 gene mutation in early-onset, colorectal signet-ring cell carcinoma. Pathol. Res. Pract. 216:152912.

Amoasii, L., E. Sanchez-Ortiz, T. Fujikawa, J. K. Elmquist, R. Bassel-Duby, and E. N. Olson. 2019. NURR1 activation in skeletal muscle controls systemic energy homeostasis. Proc. Natl. Acad. Sci. U. S. A. 116:11299–11308.

Bachinski, L. L., M. Sirito, M. Böhme, K. A. Baggerly, B. Udd, and R. Krahe. 2010. Altered MEF2 isoforms in myotonic dystrophy and other neuromuscular disorders. Muscle Nerve 42:856–863.

Baylor, S. M., and S. Hollingworth. 2011. Calcium indicators and calcium signalling in skeletal muscle fibres during excitation−contraction coupling. Prog. Biophys. Mol. Biol. 105:162–179.

Berger, M. F., and M. L. Bulyk. 2009. Universal protein-binding microarrays for the comprehensive characterization of the DNA-binding specificities of transcription factors. Nat. Protoc. 4:393–411.

Berti, F., J. M. Nogueira, S. Wöhrle, D. R. Sobreira, K. Hawrot, and S. Dietrich. 2015. Time course and side-by-side analysis of mesodermal, pre-myogenic, myogenic and differentiated cell markers in the chicken model for skeletal muscle formation. J. Anat. 227:361–382.

Bird, C. P., B. E. Stranger, and E. T. Dermitzakis. 2006. Functional variation and evolution of non-coding DNA. Curr. Opin. Genet. Dev. 16:559–564.

Black, B. L., and E. N. Olson. 1998a. Transcriptional control of muscle development by myocyte enhancer factor-2 (MEF2) proteins. Annu. Rev. Cell Dev. Biol. 14:167–196.

Black, B. L., and E. N. Olson. 1998b. Transcriptional control of muscle development by myocyte enhancer factor-2 (MEF2) proteins. Annu. Rev. Cell Dev. Biol. 14:167–196.

Boring, L., J. Gosling, S. W. Chensue, S. L. Kunkel, R. V. Farese Jr., H. E. Broxmeyer, and I. F. Charo. 1997. Impaired monocyte migration and reduced type 1 (Th1) cytokine responses in C-C chemokine receptor 2 knockout mice. J. Clin. Invest. 100:2552–2561.

Castro-Mondragon, J. A., R. Riudavets-Puig, I. Rauluseviciute, R. B. Lemma, L. Turchi, R. Blanc-Mathieu, J. Lucas, P. Boddie, A. Khan, N. Manosalva Perez, O. Fornes, T. Y. Leung, A. Aguirre, F. Hammal, D. Schmelter, D. Baranasic, B. Ballester, A. Sandelin, B. Lenhard, K. Vandepoele, W. W. Wasserman, F. Parcy, and A. Mathelier. 2022. JASPAR 2022: the 9th release of the open-access database of transcription factor binding profiles. Nucleic Acids Res. 50:D165–D173.

Chen, H., and P. C. Boutros. 2011. VennDiagram: a package for the generation of highly-customizable Venn and Euler diagrams in R. BMC Bioinformatics 12:1–7.

Chen, X., B. Gao, M. Ponnusamy, Z. Lin, and J. Liu. 2017. MEF2 signaling and human diseases. Oncotarget 8:112152.

Chin, E. R. 2010. Intracellular Ca2+ signaling in skeletal muscle: decoding a complex message. Exerc. Sport Sci. Rev. 38:76–85.

Egan, B., C.-C. Yuan, M. L. Craske, P. Labhart, G. D. Guler, D. Arnott, T. M. Maile, J. Busby, C. Henry, and T. K. Kelly. 2016. An alternative approach to ChIP-Seq normalization enables detection of genome-wide changes in histone H3 lysine 27 trimethylation upon EZH2 inhibition. PLoS One 11:e0166438.

Estrella, N. L., C. A. Desjardins, S. E. Nocco, A. L. Clark, Y. Maksimenko, and F. J. Naya. 2015. MEF2 transcription factors regulate distinct gene programs in mammalian skeletal muscle differentiation. J. Biol. Chem. 290:1256–1268.

Fang, C., J. Zhang, Y. Wan, Z. Li, F. Qi, Y. Dang, J. Li, and Y. Wang. 2021. Neuropeptide S (NPS) and its receptor (NPSR1) in chickens: cloning, tissue expression, and functional analysis. Poult. Sci. 100:101445.

Ferrari, S., D. Angells, R. Battini, and L. D. Angelis. 1997. Absence of MEF2 binding to the A/T-rich element in the muscle creatine kinase (MCK) enhancer correlates with lack of early expression of the MCK gene in embryonic mammalian muscle. Cell Growth Differ. 8:23–34.

Gertz, J., D. Savic, K. E. Varley, E. C. Partridge, A. Safi, P. Jain, G. M. Cooper, T. E. Reddy, G. E. Crawford, and R. M. Myers. 2013. Distinct properties of cell-type-specific and shared transcription factor binding sites. Mol. Cell 52:25–36.

Harney, D. F., R. K. Butler, and R. J. Edwards. 2005. Tyrosine phosphorylation of myosin heavy chain during skeletal muscle differentiation: an integrated bioinformatics approach. Theor. Biol. Med. Model. 2:1–6.

He, A., S. W. Kong, Q. Ma, and W. T. Pu. 2011. Co-occupancy by multiple cardiac transcription factors identifies transcriptional enhancers active in heart. Proc. Natl. Acad. Sci. U. S. A. 108:5632–5637.

Hsing, E.-W., S.-G. Shiah, H.-Y. Peng, Y.-W. Chen, C.-P. Chuu, J.-R. Hsiao, P.-C. Lyu, and J.-Y. Chang. 2019. TNF-α-induced miR-450a mediates TMEM182 expression to promote oral squamous cell carcinoma motility. PLoS One 14:e0213463.

Hu, H., Y. R. Miao, L. H. Jia, Q. Y. Yu, Q. Zhang, and A. Y. Guo. 2019. AnimalTFDB 3.0: a comprehensive resource for annotation and prediction of animal transcription factors. Nucleic Acids Res 47:D33–D38.

Joshi, S., G. Davidson, S. L.e Gras, S. Watanabe, T. Braun, G. Mengus, and I. Davidson. 2017. TEAD transcription factors are required for normal primary myoblast differentiation in vitro and muscle regeneration in vivo. PLoS Genet 13:e1006600.

Kaushal, S., J. W. Schneider, B. Nadal-Ginard, and V. Mahdavi. 1994. Activation of the myogenic lineage by MEF2A, a factor that induces and cooperates with MyoD. Science 266:1236–1240.

Kaya-Okur, H. S., S. J. Wu, C. A. Codomo, E. S. Pledger, T. D. Bryson, J. G. Henikoff, K. Ahmad, and S. Henikoff. 2019. CUT&Tag for efficient epigenomic profiling of small samples and single cells. Nat Commun 10:1930.

Kee, A. J., P. W. Gunning, and E. C. Hardeman. 2009. Diverse roles of the actin cytoskeleton in striated muscle. J. Muscle Res. Cell Motil. 30:187–197.

Keren, A., Y. Tamir, and E. Bengal. 2006. The p38 MAPK signaling pathway: a major regulator of skeletal muscle development. Mol. Cell. Endocrinol. 252:224–230.

King, M.-C., and A. C. Wilson. 1975. Evolution at two levels in humans and chimpanzees: their macromolecules are so alike that regulatory mutations may account for their biological differences. Science 188:107–116.

Kuokkanen, M., J. Kokkonen, N. S. Enattah, T. Ylisaukko-Oja, H. Komu, T. Varilo, L. Peltonen, E. Savilahti, and I. Jarvela. 2006. Mutations in the translated region of the lactase gene (LCT) underlie congenital lactase deficiency. Am. J. Hum. Genet. 78:339–344.

Kurihara, T., G. Warr, J. Loy, and R. Bravo. 1997. Defects in macrophage recruitment and host defense in mice lacking the CCR2 chemokine receptor. J. Exp. Med. 186:1757–1762.

Kuziel, W. A., S. J. Morgan, T. C. Dawson, S. Griffin, O. Smithies, K. Ley, and N. Maeda. 1997. Severe reduction in leukocyte adhesion and monocyte extravasation in mice deficient in CC chemokine receptor 2. Proc. Natl. Acad. Sci. U. S. A. 94:12053–12058.

Langfelder, P., and S. Horvath. 2008. WGCNA: an R package for weighted correlation network analysis. BMC Bioinformatics 9:559.

Latchman, D. S. 1997. Transcription factors: an overview. Int J Biochem Cell Biol 29:1305–1312.

Lek, M., K. G. Quinlan, and K. N. North. 2010. The evolution of skeletal muscle performance: gene duplication and divergence of human sarcomeric α-actinins. Bioessays 32:17–25.

Lin, W. H., C. J. Huang, M. W. Liu, H. M. Chang, Y. J. Chen, T. Y. Tai, and L. M. Chuang. 2001. Cloning, mapping, and characterization of the human sorbin and SH3 domain containing 1 (SORBS1) gene: a protein associated with c-Abl during insulin signaling in the hepatoma cell line Hep3B. Genomics 74:12–20.

Lin, Y., L. Chen, C. Lin, Y. Luo, R. Y. Tsai, and F. Wang. 2009. Neuron-derived FGF9 is essential for scaffold formation of Bergmann radial fibers and migration of granule neurons in the cerebellum. Dev. Biol. 329:44–54.

Liu, X., D. M. Noll, J. D. Lieb, and N. D. Clarke. 2005. DIP-chip: rapid and accurate determination of DNA-binding specificity. Genome Res 15:421–427.

Luo, W., Z. Lin, J. Chen, G. Chen, S. Zhang, M. Liu, H. Li, D. He, S. Liang, Q. Luo, D. Zhang, Q. Nie, and X. Zhang. 2021. TMEM182 interacts with integrin beta 1 and regulates myoblast differentiation and muscle regeneration. J. Cachexia Sarcopenia Muscle 12:1704–1723.

Lv, C., H. Zheng, B. Jiang, Q. Ren, J. Zhang, X. Zhang, J. Li, and Y. Wang. 2022. Characterization of relaxin 3 and its receptors in chicken: evidence for relaxin 3 acting as a novel pituitary hormone. Front. Physiol. 13:1010851.

McDermott, J. C., M. C. Cardoso, Y. T. Yu, V. Andres, D. Leifer, D. Krainc, S. A. Lipton, and B. Nadal-Ginard. 1993. hMEF2C gene encodes skeletal muscle- and brain-specific transcription factors. Mol. Cell. Biol. 13:2564–2577.

McKinsey, T. A., C. L. Zhang, and E. N. Olson. 2002. MEF2: a calcium-dependent regulator of cell division, differentiation and death. Trends Biochem. Sci. 27:40–47.

Molkentin, J. D., B. L. Black, J. F. Martin, and E. N. Olson. 1996a. Mutational analysis of the DNA binding, dimerization, and transcriptional activation domains of MEF2C. Mol. Cell. Biol. 16:2627–2636.

Molkentin, J. D., A. B. Firulli, B. L. Black, J. F. Martin, C. M. Hustad, N. Copeland, N. Jenkins, G. Lyons, and E. N. Olson. 1996b. MEF2B is a potent transactivator expressed in early myogenic lineages. Mol. Cell. Biol. 16:3814–3824.

Moody, T. W., J. M. Hill, and R. T. Jensen. 2003. VIP as a trophic factor in the CNS and cancer cells. Peptides 24:163–177.

Morin, S., F. Charron, L. Robitaille, and M. Nemer. 2000. GATA-dependent recruitment of MEF2 proteins to target promoters. EMBO J 19:2046–2055.

Moses, A. M., D. A. Pollard, D. A. Nix, V. N. Iyer, X.-Y. Li, M. D. Biggin, and M. B. Eisen. 2006. Large-scale turnover of functional transcription factor binding sites in Drosophila. PLoS Comput. Biol. 2:e130.

Nath, S. R., M. L. Lieberman, Z. Yu, C. Marchioretti, S. T. Jones, E. C. Danby, K. M. Van Pelt, G. Sorarù, D. M. Robins, and G. P. Bates. 2020. MEF2 impairment underlies skeletal muscle atrophy in polyglutamine disease. Acta Neuropathol 140:63–80.

Naya, F. J., B. L. Black, H. Wu, R. Bassel-Duby, J. A. Richardson, J. A. Hill, and E. N. Olson. 2002. Mitochondrial deficiency and cardiac sudden death in mice lacking the MEF2A transcription factor. Nat. Med. 8:1303–1309.

Nie, Y., H. Chen, C. Guo, Z. Yuan, X. Zhou, Y. Zhang, X. Zhang, D. Mo, and Y. Chen. 2017. Palmdelphin promotes myoblast differentiation and muscle regeneration. Sci. Rep. 7:41608.

Ouyang, H., Z. Wang, X. Chen, J. Yu, Z. Li, and Q. Nie. 2017. Proteomic analysis of chicken skeletal muscle during embryonic development. Front. Physiol. 8:281.

Panda, A. C., K. Abdelmohsen, J.-H. Yoon, J. L. Martindale, X. Yang, J. Curtis, E. M. Mercken, D. M. Chenette, Y. Zhang, and R. J. Schneider. 2014. RNA-binding protein AUF1 promotes myogenesis by regulating MEF2C expression levels. Mol. Cell. Biol. 34:3106–3119.

Park, P. J. 2009. ChIP−seq: advantages and challenges of a maturing technology. Nature Rev. Genet. 10:669–680.

Patro, R., G. Duggal, M. I. Love, R. A. Irizarry, and C. Kingsford. 2017. Salmon provides fast and bias-aware quantification of transcript expression. Nature Methods 14:417–419.

Potthoff, M. J., and E. N. Olson. 2007. MEF2: a central regulator of diverse developmental programs. Development 134:4131–4140.

Ramírez, F., F. Dündar, S. Diehl, B. A. Grüning, and T. Manke. 2014. deepTools: a flexible platform for exploring deep-sequencing data. Nucleic Acids Res 42:W187–W191.

Ranta-aho, J., M. Olive, M. Vandroux, G. Roticiani, C. Dominguez, M. Johari, A. Torella, J. Böhm, J. Turon, and V. Nigro. 2022. Mutation update for the ACTN2 gene. Hum. Mutat. 43:1745–1756.

Rao, Y. S., X. W. Chai, Z. F. Wang, Q. H. Nie, and X. Q. Zhang. 2013. Impact of GC content on gene expression pattern in chicken. Genet Sel Evol 45:1–7.

Sampath, S. C., S. C. Sampath, and D. P. Millay. 2018. Myoblast fusion confusion: the resolution begins. Skelet Muscle 8:1–10.

Santelli, E., and T. Richmond. 2000. Crystal structure of MEF2A core bound to DNA at 1.5 A resolution. J. Mol. Biol. 297:437–449.

Segalés, J., E. Perdiguero, and P. Muñoz-Cánoves. 2016. Regulation of muscle stem cell functions: a focus on the p38 MAPK signaling pathway. Front. Cell Develop. Biol. 4:91.

Shannon, P., A. Markiel, O. Ozier, N. S. Baliga, J. T. Wang, D. Ramage, N. Amin, B. Schwikowski, and T. Ideker. 2003. Cytoscape: a software environment for integrated models of biomolecular interaction networks. Genome Res 13:2498–2504.

Skene, P. J., and S. Henikoff. 2017. An efficient targeted nuclease strategy for high-resolution mapping of DNA binding sites. Elife 6:e21856.

Snyder, C., A. Rice, N. Estrella, A. Held, S. Kandarian, and F. Naya. 2012. MEF2A regulates the Gtl2-Dio3 microRNA megacluster to modulate WNT signaling in skeletal muscle regeneration. Development (Cambridge, England) 140:31–42.

Tang, D. D., and B. D. Gerlach. 2017. The roles and regulation of the actin cytoskeleton, intermediate filaments and microtubules in smooth muscle cell migration. Respir. Res. 18:1–12.

Taylor, M. V., and S. M. Hughes. 2017. Year. Mef2 and the skeletal muscle differentiation program. Proc. Semin. Cell Dev. Biol. 72:33–44.

Thomas-Chollier, M., C. Herrmann, M. Defrance, O. Sand, D. Thieffry, and J. van Helden. 2012. RSAT peak-motifs: motif analysis in full-size ChIP-seq datasets. Nucleic Acids Res 40:e31.

Tuerk, C., and L. Gold. 1990. Systematic evolution of ligands by exponential enrichment: RNA ligands to bacteriophage T4 DNA polymerase. Science 249:505–510.

Wales, S., S. Hashemi, A. Blais, and J. C. McDermott. 2014. Global MEF2 target gene analysis in cardiac and skeletal muscle reveals novel regulation of DUSP6 by p38MAPK-MEF2 signaling. Nucleic Acids Res 42:11349–11362.

Wang, L., C. Fan, S. Topol, E. Topol, and Q. Wang. 2003. Mutation of MEF2A in an inherited disorder with features of coronary artery disease. Science 302:1578–1581.

Wang, Z., M. Zhang, K. Li, Y. Chen, D. Cai, B. Chen, and Q. Nie. 2022. CircMGA depresses myoblast proliferation and promotes myotube formation through miR-144-5p/FAP signal. Animals 12:873.

Watanabe, N., M. Gavrieli, J. R. Sedy, J. Yang, F. Fallarino, S. K. Loftin, M. A. Hurchla, N. Zimmerman, J. Sim, X. Zang, T. L. Murphy, J. H. Russell, J. P. Allison, and K. M. Murphy. 2003. BTLA is a lymphocyte inhibitory receptor with similarities to CTLA-4 and PD-1. Nat. Immunol. 4:670–679.

Wehde, B. L., P. D. Radler, H. Shrestha, S. J. Johnson, A. A. Triplett, and K. U. Wagner. 2018. Janus Kinase 1 Plays a Critical Role in Mammary Cancer Progression. Cell Rep 25:2192–2207.

Wu, Y., and C. M. Smas. 2008. Expression and regulation of transcript for the novel transmembrane protein Tmem182 in the adipocyte and muscle lineage. BMC Res. Notes 1:1–8.

Xiang, X., H. D. Hoang, V. H. Gilchrist, S. Langlois, T. Alain, and K. N. Cowan. 2022. Quercetin induces pannexin 1 expression via an alternative transcript with a translationally active 5′ leader in rhabdomyosarcoma. Oncogenesis 11:9.

Xing, S., R. Liu, G. Zhao, L. Liu, M. A. M. Groenen, O. Madsen, M. Zheng, X. Yang, R. Crooijmans, and J. Wen. 2020. RNA-Seq analysis reveals hub genes involved in chicken intramuscular fat

and abdominal fat deposition during development. Front Genet 11:1009.

Yan, J., M. Enge, T. Whitington, K. Dave, J. Liu, I. Sur, B. Schmierer, A. Jolma, T. Kivioja, and M. Taipale. 2013. Transcription factor binding in human cells occurs in dense clusters formed around cohesin anchor sites. Cell 154:801–813.

Yang, C. C. 2000. Identification and characterization of proteins that interact with myocyte enhancer factor 2, E12, and smooth muscle LIM proteins.

Yang, R., K. K. Walder-Christensen, N. Kim, D. Wu, D. N. Lorenzo, A. Badea, Y. H. Jiang, H. H. Yin, W. C. Wetsel, and V. Bennett. 2019. ANK2 autism mutation targeting giant ankyrin-B promotes axon branching and ectopic connectivity. Proc. Natl. Acad. Sci. U. S. A. 116:15262–15271.

Yu, G., L.-G. Wang, Y. Han, and Q.-Y. He. 2012. clusterProfiler: an R package for comparing biological themes among gene clusters. OMICS 16:284–287.

Yu, G., L. G. Wang, and Q. Y. He. 2015. ChIPseeker: an R/Bioconductor package for ChIP peak annotation, comparison and visualization. Bioinformatics 31:2382–2383.

Zhang, J., X. Wang, C. Lv, Y. Wan, X. Zhang, J. Li, and Y. Wang. 2022a. A gene expression atlas of Lohmann white chickens. bioRxiv 2022.2007. 2030.500160.

Zhang, X., J. Su, T. Huang, X. Wang, C. Wu, J. Li, J. Li, J. Zhang, and Y. Wang. 2022b. Characterization of the chicken melanocortin 5 receptor and its potential role in regulating hepatic glucolipid metabolism. Front. Physiol. 13: 917712.